

# RESOLVING 4D OVERBURDEN CHANGES WITH FULL-WAVEFORM INVERSION

O. Bukola<sup>1</sup>, B. Xiao<sup>1</sup>, J. Sinden<sup>1</sup>, E. Miller<sup>2</sup>, P. Nevill<sup>2</sup>, L. Novakovic<sup>3</sup>

<sup>1</sup> CGG; <sup>2</sup> Chevron Technology Centre; <sup>3</sup> Chevron North America Exploration and Production Company

## Summary

---

4D time-lapse seismic imaging is typically performed using the same velocity model to migrate the baseline and monitor data. However, in complex cases where one producing reservoir sits above another, significant changes in the properties of the overlying reservoir can result in a 4D signal with associated 4D coda immediately below it, which would mask the 4D signal of reservoirs underneath. Resolving such an issue requires that the baseline and monitor data be migrated with separate models. We demonstrate how we have used a visco-acoustic full-waveform inversion to resolve 4D changes in velocity and absorption within an overburden gas-charged channel. The resulting 4D image shows minimisation of 4D coda below the overburden channel and the unveiling of 4D signals at deeper targets of interest.

## Resolving 4D overburden changes with full-waveform inversion

### Introduction

4D time-lapse seismic processing is usually performed with the objective of identifying and quantifying changes within target reservoirs. The standard processing practice is to migrate the baseline and monitor data using the same velocity model and to generate a 4D image for analysis. However, in a complex field architecture, where one producing reservoir sits above another, significant changes in the properties of the overlying reservoir can result in a 4D signal with associated 4D coda immediately below it. This can mask the 4D signals of reservoirs underneath. This problem is more pronounced when the 4D change is so strong that it generates an associated velocity and fluid content change, manifested by different velocity ( $V_P$ ) and absorption (quantified by the Quality Factor “Q”). Such imaging challenges necessitate the need to migrate the baseline and monitor data using separate  $V_P$  and Q models.

A convenient and simple way of creating separate models for migrating the monitor data is to derive a perturbed version of the baseline velocity model using time shift measurements between the baseline and monitor images (Chu et al., 2011); however, this suffers from the limitation of a 1D assumption. Full-waveform inversion (FWI) offers an advanced approach for creating velocity models of the earth, and various schemes of applying FWI in time-lapse processing have been proposed. Plessix et al. (2010) along with Queißer and Singh (2010) proposed a scheme of inverting from the same starting model for baseline and monitor velocities in parallel, using the baseline and monitor data, respectively. This parallel scheme is vulnerable to noise contamination, depending on how different the separately inverted velocities converge to a minima. To minimise the noise, various schemes have been studied, which try to couple the baseline and monitor inversions either by inverting for the monitor model from a starting baseline model using the monitor data (Routh et al., 2012), the base-monitor difference data (Zheng et al., 2011; Zhang and Huang, 2013), a common model approach (Hicks et al., 2016), or introducing 4D cost functions in their inversions (Maharramov and Biondi, 2014).

This paper describes how we have modified the parallel FWI method by 4D binning the baseline and monitor data, which is done prior to using them in separate FWI updates to invert for overburden changes within a shallow reservoir overlying a primary target reservoir. This improved repeatability of the data sets should reduce acquisition-related artefacts in the parallel FWI updates and minimise 4D FWI noise. Outside of the channel geo-body defining this shallow reservoir, a common background model is inverted using both the baseline and monitor data. Moreover, this paper also explores the necessity of updating  $V_P$  and Q for time-lapse imaging, where fluid content changes are significant. In both inversions, for the overburden change and the background model, a 2-parameter joint FWI (Xiao et al., 2018) for  $V_P$  and Q was performed.

### Field overview

In order to improve reservoir management and optimise hydrocarbon production, the field operators of an oil block offshore West Africa decided to employ ocean bottom node (OBN) seismic to perform 4D monitoring of the fields. The baseline OBN survey was conducted in 2013 with a 30 m by 30 m shot sampling and 1,626 Trilobit nodes with an imaging target covering 77.6 km<sup>2</sup>. In contrast, the monitor OBN was conducted in 2019 with a 30 m by 60 m shot sampling and 982 Case Abyss nodes with an imaging target of 39.5 km<sup>2</sup>. The number of receivers used for the monitor acquisition was reduced due to the decision to narrow the coverage to the 4D area of interest.

In 2015, the earliest discovered field in the block (which was also the shallowest) was abandoned, and its production wells were shut. From that time until 2019 (when the OBN monitor survey was conducted), a large amount of gas in the reservoirs of the shallow abandoned field has gone into solution. This caused a significant change in the gas content of the reservoir between the baseline and monitor OBN acquisitions. Migrating the baseline and monitor OBN data with the same velocity model and generating a 4D image showed a strong 4D coda below the abandoned shallow field, masking the desired 4D response of deeper targets. In order to resolve the 4D coda,  $V_P/Q$  joint FWI was used to create separate  $V_P$  and Q models for migrating the baseline and monitor data, respectively.

## Strategy of applying FWI for overburden 4D

The starting velocity model was created from a smoothed, pre-existing, legacy velocity model. In addition, the starting Q model was created with a constant value of 175 and a reference frequency of 80 Hz based on information obtained from legacy processing. The model building workflow is illustrated in Figure 1 and was performed in three steps: 1) a coupled  $V_P/Q$  joint FWI update using all the available data, 2) a parallel  $V_P/Q$  joint FWI update using 4D binned data, and 3) a final step of merging the resulting models from the coupled and parallel FWI updates.

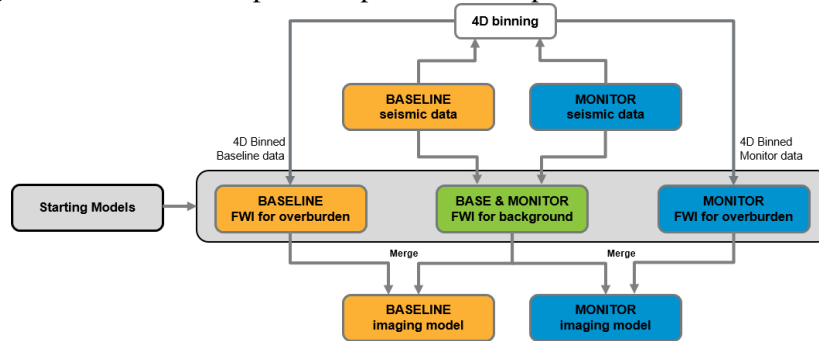


*Figure 1 Model building workflow*

In the first step, we take advantage of all the shots recorded in both baseline and monitor OBN acquisitions to drive a diving-wave FWI update for high-resolution common background models (green background in figure 1). This allows the incorporation of redundant nodes from the baseline survey not used in 4D imaging and long offset data (up to 17.5 km) into the FWI. This achieves a diving wave penetration depth of 2.5 km to 2.8 km, which covers most of the reservoirs. A  $V_P/Q$  joint FWI was run to update the starting model in iterations from 2.0 Hz to 9.4 Hz. For pragmatic reasons, above 9.4 Hz, we switched from  $V_P/Q$  joint FWI to  $V_P$ -only FWI honouring the 9.4 Hz Q model and further updated the velocity to a frequency of 15 Hz. Only the  $V_P$  model from this step is subsequently used. Multi-parameter FWI remains a challenging problem mostly due to the cross-talk between inverted parameters. In our workflow, separate gradients of the objective function for  $V_P$  and Q computation were implemented in the joint inversion algorithm to reduce cross-talk (Wang et al., 2018). Also, in low velocity/strong absorption scenarios, the kinematics in time domain work in the same direction, hence providing more scope of reducing cross-talks, compared to other scenarios (Xiao et. al, 2018).

In the second step, we return to the starting models and perform FWI updates separately for the baseline and monitor data to create separate  $V_P$  and Q models for each. The baseline and monitor data were 4D binned to retain only common bin traces and eliminate some acquisition related differences, including fold, offset and shot carpet density, hence removing their illumination differences in the FWI update. These were used in parallel flows to drive a  $V_P/Q$  joint FWI update in iterations from 2.0 Hz to 9.4 Hz, followed by  $V_P$ -only FWI update to 15 Hz, honouring the 9.4 Hz Q model.

In the third step we merge the  $V_P$  model (from step 2), within the channel defining the shallow reservoir, for the respective baseline and monitor data, into the high-resolution background  $V_P$  model from step 1. The Q models (from step 2) within the channel defining the shallow reservoir for the baseline and monitor were inserted into a constant background Q of 175.

## Results

Figure 2 shows depth slice images of the resulting  $V_P$  and Q models through the shallow reservoir for the baseline and monitor data, respectively. Models inverted with the baseline data show slow velocity and strong Q absorption within the channel body. In contrast, the models inverted with the monitor data show relatively faster velocity, and milder Q absorption. This observation is in agreement with the hydrocarbon production history from reservoirs in the channel. From 2013 until 2015, when the field was abandoned, there was significant gas injection into the shallow reservoir in order to support secondary oil recovery. By the time of the monitor OBN acquisition in 2019, a significant amount of the injected gas had gone into solution.

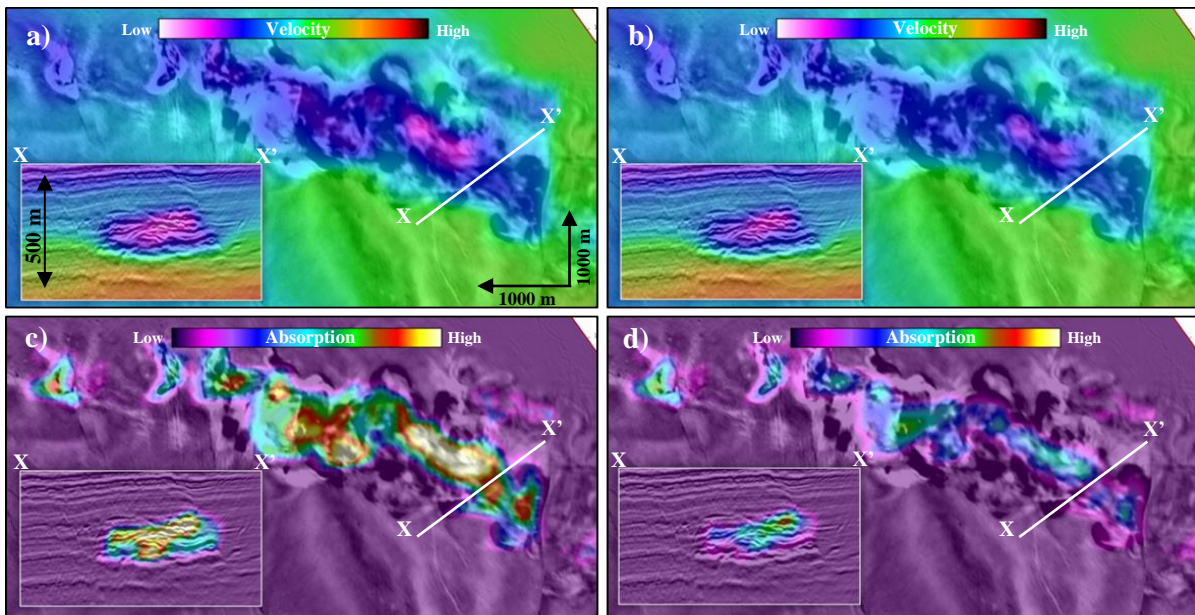


**Figure 2** Depth slice at 1600 m through the shallow overburden channel showing seismic overlay of: (a) baseline  $V_P$ , (b) monitor  $V_P$ , (c) baseline  $Q$ , and (d) monitor  $Q$ .

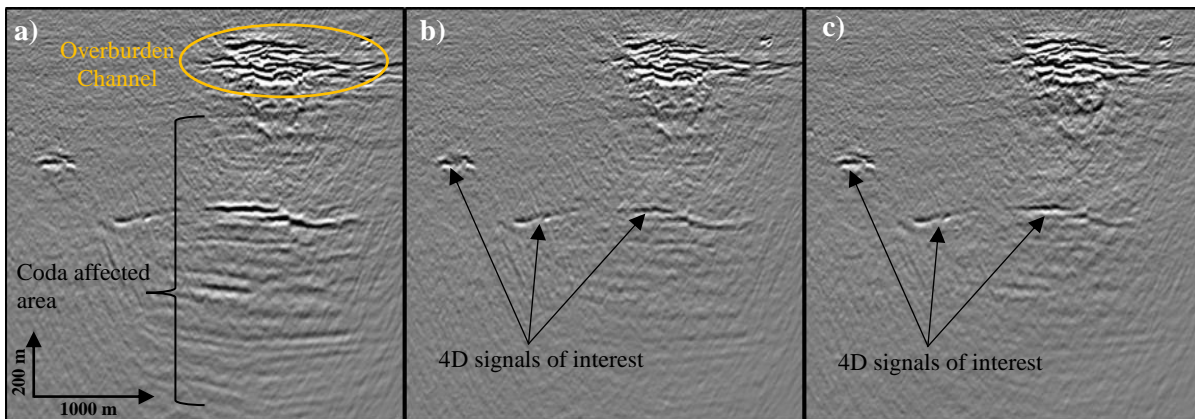


**Figure 3** Inline section of 4D image: (a) without resolving 4D coda below overburden channel. (b) with 4D coda resolved using time alignment (c) with 4D coda resolved using  $V_P/Q$  joint FWI for 4D.

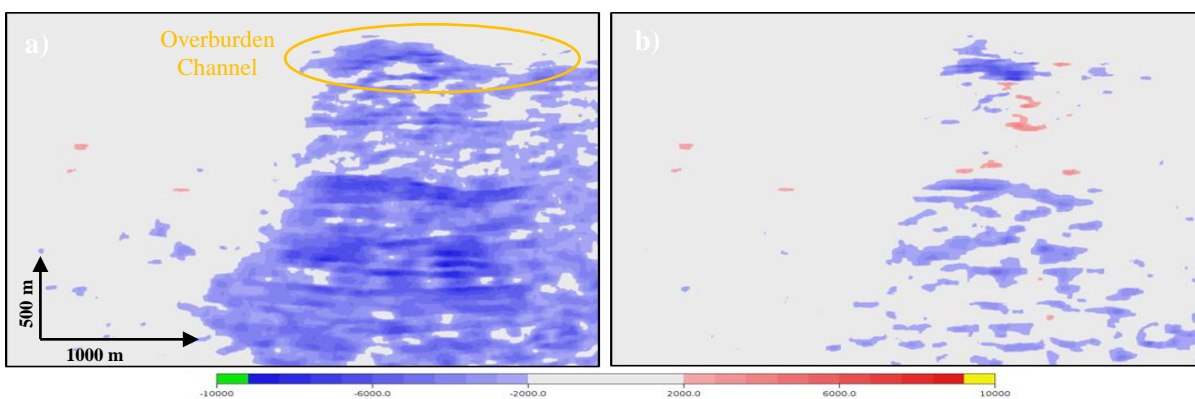


**Figure 4** Inline section of 4D time-shift (in microseconds) attribute: (a) without resolving 4D coda below overburden channel. (b) with 4D coda resolved using  $V_P/Q$  joint FWI for 4D.

Figure 3a shows the 4D image generated when the baseline and monitor data are migrated using the high-resolution common background  $V_P$  model derived in step 1 of the FWI flow and a constant  $Q$  model. As in standard practice, a global amplitude and phase matching operator was applied post-stack to the monitor data, prior to generating the 4D image. Without resolving the 4D change within the overburden channel, the 4D image is contaminated by 4D coda below the channel, masking 4D signal

of interest. Figure 3b shows the result of applying post stack time alignment to resolve the 4D coda in figure 3a. Lastly, figure 3c shows the 4D image generated when the baseline and monitor data are migrated with their respective  $V_P$  and Q models derived in step 3 of the FWI flow, without post stack time alignment applied. The 4D coda is minimised in figures 3b and 3c; however, results in figure 3c are driven by a more deterministic approach to resolving the visco-acoustic changes in the shallow channel.

Figure 4a shows the 4D time shift computed between base and monitor data migrated with the same model. In contrast, Figure 4b shows the 4D time shift computed between base and monitor data migrated with their respective  $V_P$  and Q models. Time shift (up to 8 ms) observed below the overburden channel in figure 4a has been minimised in figure 4b. This arises as a result of using separate baseline and monitor migration models, indicating a relatively accurate velocity model was derived for each vintage through this workflow.

## Conclusions

We have applied  $V_P/Q$  joint FWI to resolve 4D overburden changes in the visco-acoustic properties of a shallow reservoir overlying deeper target reservoirs. This was achieved in the imaging domain by creating separate  $V_P$  and Q models for migrating the baseline and monitor data, respectively, rather than the conventional data-domain approach of post-stack time alignment. 4D results indicate that the  $V_P$  and Q models derived from the proposed flow are reasonable. Nonetheless, cross-talk in multi-parameter FWI remains a challenging subject, and the uncertainty of the derived models could be still large.

## Acknowledgements

We thank Chevron, their Partners and CGG for permission to publish. We also thank Zhaoyu Jin and Tommaso Altieri, who were part of the processing team, and Andrew Ratcliffe, Ramez Refaat and Richard Jupp for constructive feedback and support provided in the course of carrying out this work.

## References

- Chu, D., Burger, J., and Medema, G. [2011] Using time strain volume for improved 4D interpretation: methods and case studies. *81<sup>st</sup> Annual SEG Meeting*, Extended Abstracts, 4140-4143.
- Hicks, E., Hoerber, H., Houbiers, M., Pannetier Lescoffit, S., Ratcliffe, A., and Vinje, V. [2016] Timelapse full-waveform inversion as a reservoir monitoring tool – a North Sea case study. *The Leading Edge*, **35**(10), 850-858.
- Maharramov, M., and Biondi, B. [2014] Joint full-waveform inversion of time-lapse data sets. *84<sup>th</sup> Annual SEG meeting*, Expanded Abstracts, 954-959.
- Plessix, R.-E., Michelet, S., Rynja, H., Kuehl, H., Perkins, C., J. W.de Maag, and Hatchell, P. [2010] Some 3D applications of full waveform inversion: *72<sup>nd</sup> EAGE Conference and Exhibition*, Workshops and Fieldtrips, Session: WS6 3D Full Waveform Inversion – A Game Changing Technique?
- QueiBer, M., and Singh, S. C. [2010] Time-lapse seismic monitoring of CO<sub>2</sub> sequestration at Sleipner using time domain 2D full waveform inversion: *80<sup>th</sup> Annual SEG Meeting*, Expanded Abstracts, 2875–2878.
- Routh, P., Palacharla, G., Chikichev, I., and Lazaratos, S. [2012] Full wavefield inversion of time-lapse data for improved imaging and reservoir characterization: *82<sup>nd</sup> Annual SEG Meeting*, Expanded Abstracts, 1-6.
- Wang, M., Xie, Y., Xiao, B., Ratcliffe, A., and Latter, T. [2018] Visco-acoustic full-waveform inversion in the presence of complex gas clouds. *88<sup>th</sup> Annual SEG Meeting*, Expanded Abstracts, 5516-5520.
- Xiao, B., Ratcliffe, A., Latter, T., Xie, Y. and Wang, M. [2018] Inverting for near-surface absorption with full-waveform inversion: a case study from the North Viking Graben in the northern North Sea. *80<sup>th</sup> EAGE Conference and Exhibition*, Extended Abstracts, A12 03.
- Zhang, Z., and Huang, L. [2013] Double-difference elastic-waveform inversion with prior information for time-lapse monitoring. *Geophysics*, **78**(6), R259–R273.
- Zheng, Y., Singh, S., and Barton, P. [2011] Strategies for elastic full waveform inversion of time-lapse ocean bottom cable (OBC) seismic data. *81<sup>st</sup> annual SEG meeting*, Expanded Abstracts, 4195-4200.